FLUIDMECHANICS OF BENIGN PAROXYSMAL POSITIONAL VERTIGO (BPPV)

Dominik Obrist
Institute of Fluid Dynamics,
ETH Zurich
Sonneggstr. 3, 8092 Zürich, Switzerland
obrist@ifd.mavt.ethz.ch

Stefan Hegemann
Department of Otorhinolaryngology,
University Hospital Zurich
Frauenklinikstr. 24, 8091 Zürich, Switzerland
stefan.hegemann@usz.ch

ABSTRACT

Particulate flow in the semicircular canals of the inner ear is suspected to be the most common cause for vertigo. This pathologic condition is known as benign paroxysmal positional vertigo (BPPV). We propose an analytical model for this flow configuration which consists of an equation for the fluid flow and of an equation of motion for the particles including the appropriate Stokes drag and gravitational forces. A modal analysis of the linearized equations suggests a reduced-order model for BPPV constructed from the two least stable modes. A Stokes number, formed with the eigenvalues of these two modes, is shown to be an important parameter in BPPV. We derive explicit expressions that connect the particle and canal properties directly to the onset, strength and duration of the vertigo.

INTRODUCTION

The semicircular canals (SCC) are the primary human sensors for angular motion. They are part of the vestibular organ in the inner ear (figure 1). The SCCs are filled with a fluid called the *endolymph*. Angular movements of the head induce a flow of the endolymph. This flow deflects a flexible gelatinous structure called the *cupula*. The deflection of the cupula triggers nerve signals. These signals lead to a compensatory eye movement which is called the *nystagmus*. The nystagmus allows us to remain focused on an object even while we are in motion.

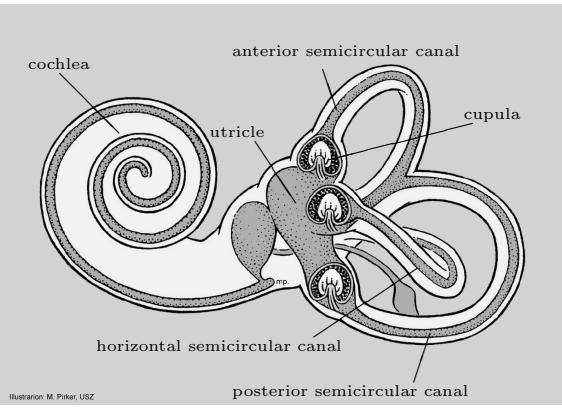

Figure 1: The human vestibular organ.

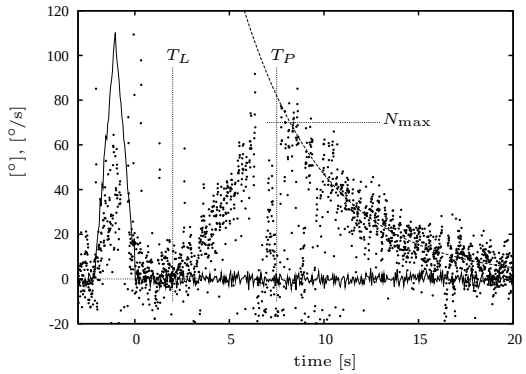

Figure 2: Clinical measurements of the nystagmus and head velocity of a BPPV patient (canalithiasis) during and after a head maneuver (—— head velocity; • nystagmus velocity N measured by tracking the eye movement).

SCCs may contain small calcite particles (e.g., because of a head trauma or as a consequence of aging). These free-floating particles disturb the endolymph flow and lead to faulty signals from the cupula (which results in a pathological nystagmus). This medical condition is known as benign paroxysmal positional vertigo (BPPV). It is the cause for 30% of all vertigo syndromes in humans. The particles are either floating freely in the SCC (canalithiasis) or they adhere to the cupula (cupulolithiasis). The present work focuses solely on canalithiasis.

In clinical experiments the nystagmus velocity is measured during and after a well-defined angular maneuver of the head. It is symptomatic for canalithiasis patients that the per-rotatory nystagmus (i.e., the regular nystagmus which compensates for the angular head maneuver) is followed by a short latency period ($0 < t < T_L$) and then a second pathological nystagmus called *positional nystagmus* (figure 2). The intensity of the nystagmus peaks at $t = T_P$ (typically 5 to 10s) and then decays slowly. During the positional nystagmus BPPV patients have the impression that they are spinning again (in the same direction) even though they are at rest. This leads to vertigo, dizziness and nausea.

Only little is known about the exact mechanisms that govern BPPV (Rajguru *et al.*, 2005, 2004; Squires *et al.*, 2004). We present a new analytical model for BPPV based

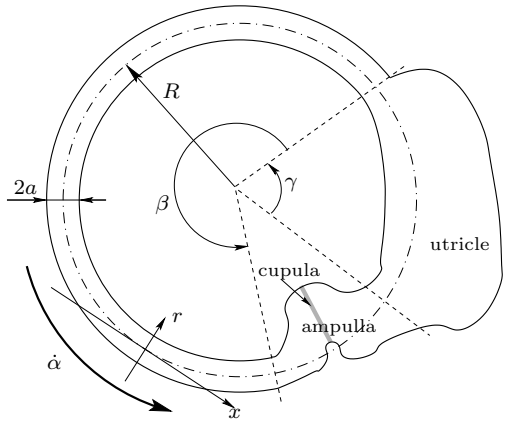

Figure 3: Schematic diagram of a semicircular canal.

on particulate flow in a duct. This model allows us to understand the underlying mechanisms of BPPV. Further, the model yields the relevant dimensionless numbers for this flow configuration, which helps us to understand the influence of geometrical and physical parameters on BPPV.

ENDOLYMPH FLOW IN SEMICIRCULAR CANALS

The flow of the endolymph in a single SCC is described by the model of Van Buskirk *et al.* (1976). Angular head movements, described by the angle $\alpha(t)$, are constricted to the plane of the SCC. This model considers the viscous flow in the slender part of the duct which spans an angle β and has a constant circular cross-section $A_c = \pi a^2$ (Figure 3). The radius of the cross-section a is much smaller than the major radius R of the torus and centrifugal effects can be neglected. The flow in the utricle (which spans the angle γ) enters the equation only in the form of the inertial force of the fluid contained in the utricle. The cupula is modeled by a restoring force which is proportional to the volume displacement $V(t)$ of the cupula. For the scope of our work we assume that the volume displacement V is proportional to the nystagmus velocity N. We can compute the volume displacement from the axial endolymph velocity $u(r,t)$ with

$$V(t) = 2\int_0^1 u(r',t)r'\,\mathrm{d}r' \tag{1}$$

All variables are non-dimensionalized with respect to the viscous time scale $T_{\mathrm{ref}} = a^2/\nu$, the canal radius a as reference length, and R/T_{ref} as reference velocity, respectively. The velocity $u(r,t)$ is measured relative to the canal. Relative to the inertial system the endolymph velocity is $u + \dot{\alpha}$.

Under these assumptions the axial component of the Navier–Stokes equations for the flow in the SCC can be written as (Van Buskirk *et al.*, 1976)

$$\ddot{u} - \frac{1}{\tilde{r}}\frac{\partial}{\partial r}\left(r\frac{\partial}{\partial r}\dot{u}\right) + \epsilon\int_0^1 u(r',t)\,r'\mathrm{d}r' = -(1+\gamma/\beta)\ddot{\alpha} \tag{2a}$$

with the boundary conditions

$$u(r=1) = \frac{\partial}{\partial r}u(r=0) = 0 \tag{2b}$$

The dimensionless coefficient ϵ is a measure for the cupula stiffness, i.e., the dimensionless form of the proportionality constant K that relates the cupula displacement V to the reactive force of the cupula on the fluid. It is defined as

$$\epsilon = \frac{2A_cKT_{\mathrm{ref}}^2}{\rho\beta R} \tag{3}$$

The ansatz $u(r,t) = \hat{u}(r)e^{-\sigma t}$ yields the eigensolutions of (2). All modes are stable and non-oscillatory (Obrist, 2006). The least stable mode is directly related to the mechanical properties of the cupula and is named *cupula mode*. The decay rate of this mode corresponds to the so-called *time constant of the SCC* (4.2 s in man). The eigenvalue of the cupula mode is approximately given by

$$\sigma_c \approx \epsilon/16 \tag{4}$$

The shape of its eigenfunction is close to the parabola $1-r^2$. The other modes depend only weakly on the properties of the cupula. They are called *duct modes*. Their eigenvalues are approximately given by $\sigma_{d,k} \approx \lambda_k^2$ where λ_k is the k-th root of the Bessel function J_0. The corresponding eigenfunctions are the formed by the Bessel function $J_0(r')$.

With a modal expansion of u it can be shown (Obrist, 2006) that the cupula displacement is given by

$$V(t) \quad \sim \quad \left[\dot{\alpha}(t) \;-\; \sigma_c\int_0^\infty \dot{\alpha}(t \;-\; \tau)e^{-\sigma_c\tau}\,\mathrm{d}\tau\right] \tag{5}$$

This equation is approximate in the sense that it gives inaccurate results for head maneuvers with angular velocities $\dot{\alpha}$ that change very rapidly with respect to the decay rates of the duct modes. For most natural head maneuvers (5) is sufficiently accurate.

Equation (5) is evidence that SCCs are indeed good sensors for angular motion, since it shows that $V \propto \dot{\alpha}$ apart from the so-called *velocity error*

$$\dot{\alpha}_e \equiv -\sigma_c\int_0^\infty \dot{\alpha}(t-\tau)e^{-\sigma_c\tau}\mathrm{d}\tau \tag{6}$$

The velocity error leads to an overshoot in the cupula displacement at the end of a head maneuver (cupula swinging back beyond its relaxed state). If the velocity error is strong enough it leads to a sensation of reverse angular motion when the rotation is suddenly stopped.

MODEL FOR BPPV

To model BPPV we must augment Van Buskirk's equation (2) by an equation for the particle motion. We use a particle model which is similar to the model used by Rajguru *et al.* (2004).

We assume that a certain number n_p of spherical particles of radius a_p with mass m_p at the axial location $x_p(t)$. (Note that the actual number of particles in the SCCs of BPPV patients is not known.) The axial location is measured relative to the moving canal and it is non-dimensionalized with respect to the major canal radius R. The origin $x_p = 0$ is set to the (initially) lowest point in the canal such that we may assume the initial conditions

$$x_p(0) = \dot{x}_p(0) = 0 \tag{7}$$

We assume that the particles are equally distributed (in a statistical sense) across the duct cross-section.

The particle equation of motion,

$$m_pR(\ddot{x}_p + \ddot{\alpha}) = F_s + F_g \tag{8}$$

includes a term for the particle inertia $m_p(\ddot{x}_p + \ddot{\alpha})$ and two terms for external forces that act upon the particle. The external forces consist of the gravitational force,

$$F_g = -m_p(1 - \rho/\rho_p)g\sin(x_p + \alpha) \tag{9}$$

and a drag force

$$F_s = -6\pi\nu\rho a_p(\dot{x}_p - u_p) \tag{10}$$

which corresponds to the Stokes drag of a sphere of radius a_p. Since we do not track the radial position of the particle we approximate the fluid velocity u_p by the bulk velocity $\bar{u}$ of the fluid.

At the same time we introduce the Stokes drag (10) into the fluid equation (2). Here we assume that the Stokes drag F_s of a single particle induces a body force $-F_s/(A_c\beta R)$. Therefore, all n_p particles together exert a total body force $-n_pF_s/(A_c\beta R)$ on the fluid, whereas each particle by itself satisfies the particle equation (8).

This yields the governing equations for the particulate flow in a SCC, i.e., an analytical model for BPPV:

$$\ddot{u} - \frac{1}{\tilde{r}}\frac{\partial}{\partial r}\left(r\frac{\partial}{\partial r}\dot{u}\right) + \epsilon\int_0^1 u\,r'\mathrm{d}r' + \chi\left(2\int_0^1 \dot{u}\,r'\mathrm{d}r' - \ddot{x}_p\right) = -(1+\gamma/\beta)\ddot{\alpha} \tag{11a}$$

$$\ddot{x}_p + \xi\left(\dot{x}_p - 2\int_0^1 u\,r'\mathrm{d}r'\right) + \frac{1}{Fr^2}\sin(x_p+\alpha) = -\ddot{\alpha} \tag{11b}$$

with the initial and boundary conditions

$$u(r,0) = \dot{u}(r,0) = x_p(0) = \dot{x}_p(0) = 0 \tag{12a}$$

$$u(1,t) = \frac{\partial}{\partial r}u(0,t) = 0 \tag{12b}$$

Apart from the stiffness coefficient ϵ these equations contain three new dimensionless coefficients Fr^2, ξ and χ. The Froude number Fr is defined as

$$Fr^2 = \frac{R}{gT_{\mathrm{ref}}^2(1-\rho/\rho_p)} \tag{13}$$

The coefficient ξ reflects the inverse of the particle relaxation time, whereas the coefficient χ determines the particle-fluid coupling. They are defined as

$$\xi = \frac{9\rho a^2}{2\rho_p a_p^2} \qquad \chi = \frac{3a_pn_p}{\beta R} \tag{14}$$

Typical values for the physical parameters can be found in table 1.

The governing equations (11) form a system of inhomogeneous partial integro-differential equations. In the term for the cupula reaction force and in the terms for the Stokes drag we find integral operators of Fredholm type. The gravity term in (11b) introduces a nonlinearity to this system. In the following section we will explain the basic mechanisms of BPPV by computing numerical solutions of (11). Then, a modal analysis of the linearized governing equations will provide us with a deeper understanding of the influence of the various physical parameters, e.g., the canal geometry, on the symptoms of BPPV.

BASIC MECHANISMS OF BPPV

We solve the governing equations (11) numerically by using a mixed implicit/explicit time integration scheme and finite differences for the discretization of the spatial derivatives.

Table 1: Typical physical and geometrical parameters (values from Van Buskirk *et al.* (1976) and Squires *et al.* (2004)).

description		value
major canal radius	R	3.2×10^{-3} m
duct radius	a	1.6×10^{-4} m
angle spanned by the duct	β	1.4π
angle spanned by the utricle	γ	0.42π
cupular stiffness	K	13 GPa/m^3
endolymph density	ρ	10^3 kg/m^3
endolymph viscosity	ν	10^{-6} m^2/s
particle density	ρ_p	2.7×10^3 kg/m^3
particle radius	a_p	$0.5-25\mu$m

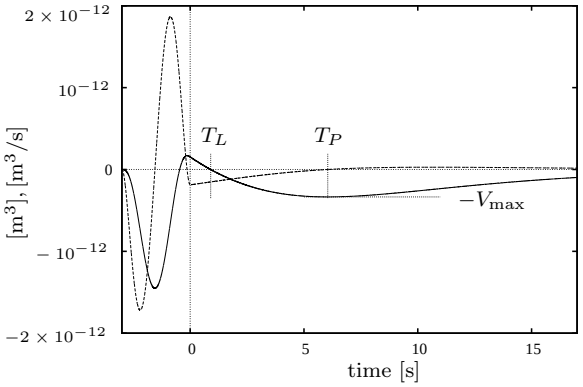

Figure 4: Numerical solution of (11) for $n_p = 7$ and $a_p = 14\mu$m; —— (dimensional) cupula displacement V, – – – (dimensional) volume flow $\dot{V} \propto \bar{u}$.

Figure 4 shows a typical solution of (11) for the head maneuver from 0° (upright) to −120° (supine). This head maneuver is part of the Dix-Hallpike maneuver, which is a diagnostic maneuver for clinical testing. The same maneuver was also used to obtain figure 2.

During the head maneuver (per-rotatory phase, $t < 0$) the cupula displacement $V(t)$ follows qualitatively the head velocity $\dot{\alpha}(t)$. Immediately after the head maneuver has ended ($t = 0$) there is an overshoot, i.e., the cupula has swung past its relaxed state and is deflected to the opposite side. The magnitude of this overshoot corresponds to the velocity error (6). Up to this point the solution is qualitatively the same as it is for the healthy (particle-free) SCC. In the post-rotatory phase ($t > 0$) the cupula displacement $V(t)$ crosses the zero axis a second time at $t = T_L$. It only returns to its relaxed position after it has reached a local extremum $-V_{\max}$ at $t = T_P$. This corresponds to the positional nystagmus that is observed with canalithiasis patients. The second crossing of the zero axis and the subsequent local extremum of the cupula displacement is perceived as a secondary angular motion and causes vertigo.

The results shown in Figure 4 are shown again in Figure 5 as a sequence of schematic drawings. It documents the two-phase process of canalithiasis: particle positioning during the per-rotatory phase and gravity-driven flow during the post-rotatory phase which is induced by the falling particles.

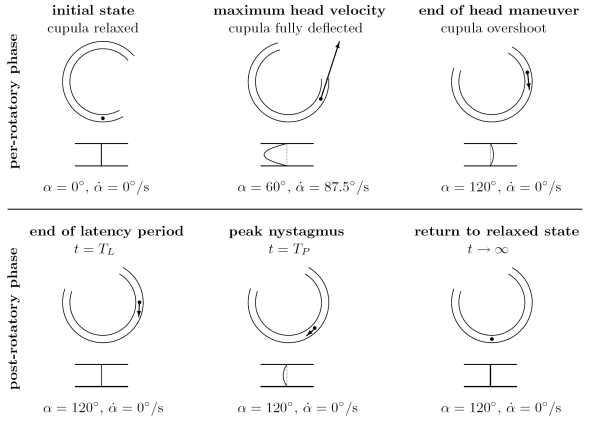

Figure 5: Schematic drawings of the semicircular canal with particles ($a_p = 11\mu$m, $n_p = 10$) during a head maneuver (the arrow shows the particle velocity $\dot{x}_p + R\dot{\alpha}$; the cupula is drawn separately below the canal as a bulged membrane).

MODAL ANALYSIS

We can obtain a deeper understanding of BPPV from a modal analysis of the governing equations (11). To this end, we replace the trigonometric term in the particle equation (11b) by $x_p + \alpha$. Although this approximation may introduce a sizable error for angles of 90° and more, we will see that the results obtained from the linearized problem remain qualitatively correct.

We write the linearized governing equations (11) in matrix form as

$$\frac{\partial}{\partial t}\mathbf{Q}\mathbf{u} = \mathbf{P}\mathbf{u} + \mathbf{f} \tag{15}$$

where $\mathbf{u}(r,t) = (u(r,t), \dot{u}(r,t), x_p(t), \dot{x}_p(t))^T$.

To obtain an eigenvalue problem we drop the forcing $\mathbf{f}$ and make the ansatz

$$\mathbf{u}(r,t) = \hat{\mathbf{u}}(r)e^{-\sigma t} \tag{16}$$

with $\hat{\mathbf{u}} = (\hat{u}(r), -\sigma\hat{u}(r), \hat{x}_p, -\sigma\hat{x}_p)^T$. This gives the generalized eigenvalue problem for BPPV

$$-\sigma\mathbf{Q}\hat{\mathbf{u}} = \mathbf{P}\hat{\mathbf{u}} \tag{17}$$

with the boundary conditions $\hat{u}(1) = \partial/\partial r\, \hat{u}(0) = 0$.

A numerically computed spectrum is shown in figure 6. Apart from two new eigenvalues (the slow and the fast particle mode) the spectrum looks almost the same as the spectrum of the endolymph flow without particles. This suggests that we can find approximate expressions for the eigenvalues by decoupling the linearized governing equations.

We obtain decoupled equations by dropping the term for the Stokes drag from the fluid equation (since $\chi \ll 1$) and by neglecting the contribution of u in the particle equation (assuming that $|\hat{u}| \ll |\dot{x}_p|$). With these simplifications we have eliminated the two-way coupling from our model.

The decoupled fluid equation is equivalent to van Buskirk's equation (2a). The corresponding eigenvalue spectrum was discussed extensively by Obrist (2006) and the results were summarized above.

The decoupled homogeneous form of the particle equation (11b) has the simple form

$$\ddot{x}_p + \xi\dot{x}_p + Fr^{-2}x_p = 0. \tag{18}$$

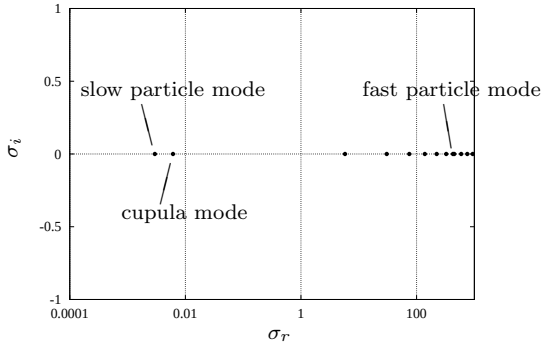

Figure 6: Eigenvalue spectrum for $\epsilon = 0.09752$, $\xi = 426.667$, $\chi = 2.13154\times10^{-2}$ and $Fr^2 = 0.7905$ ($n_p = 10$, $a_p = 10\mu$m).

This equation yields two particle modes,

$$\sigma_s = \frac{1}{Fr^2\xi}, \qquad \sigma_f = \xi. \tag{19}$$

According to their decay rate we name them the *slow particle mode* σ_s and the *fast particle mode* σ_f. As noted earlier, the fast particle eigenvalue $\sigma_f = \xi$ corresponds to the inverse of the particle relaxation time.

The slow particle mode decays much slower (on the order of seconds). Its eigenvalue lies close to the eigenvalue σ_c of the cupula mode. This suggests that BPPV (which is a relatively slow process) is mainly governed by the slow particle mode and the cupula mode. We define a Stokes number St which relates a typical time constant for the particle motion $(1/\sigma_s)$ to a typical time constant of the fluid flow $(1/\sigma_c)$.

$$St \equiv \frac{\epsilon Fr^2\xi}{16} = \frac{9\pi K a^4}{16\beta\, a_p^2\, g(\rho_p - \rho)}. \tag{20}$$

For typical values of ϵ, ξ and Fr we find that St may be below as well as above unity. For the parameters given in table 1 the critical particle size where $St = 1$ is 14.3μm. We will see in the following that St plays an important role in BPPV.

Before we continue we would like to point out that the expressions in (19) are just approximations to the eigenvalues of (15). Moreover, a numerical evaluation of the eigenvalues for different Stokes numbers (figure 7) reveals that the cupula mode and the slow particle mode actually switch roles as St passes through unity, i.e., the eigenvalue σ_s follows the expression (19) for $St > 1$, but approaches $\epsilon/16$ for $St < 1$ (and vice versa for σ_c). We also conclude from this figure that the slow particle mode decays slower than the cupula mode for all choices of St.

REDUCED-ORDER MODEL FOR BPPV

During the post-rotatory phase, i.e., after the head maneuver has ended, the forcing $\mathbf{f}$ in (15) is zero. Therefore, the post-rotatory phase can be considered an initial value problem with a solution governed by the eigensolutions from the previous section. The initial conditions are the endolymph velocity, the cupula displacement, and the particle position and velocity at $t = 0$ which are a direct result of the head maneuver.

We build a reduced-order model for the post-rotatory phase from the slow particle mode and the cupula mode since these are the only two eigenmodes that will prevail after a few microseconds. Although both modal solutions decay in time, we can obtain transient growth if the eigenfunctions

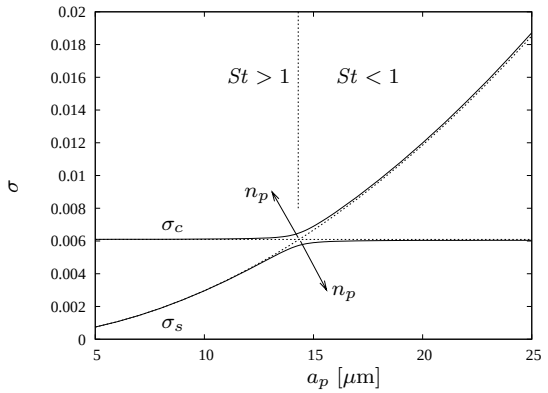

Figure 7: Eigenvalues σ_s and σ_c as a function of the particle radius a_p (n_p=10); the dotted lines show $\epsilon/16$ and $1/(Fr^2\xi)$.

are not orthogonal to each other. We can confirm this by numerically computing the eigenfunctions. As a matter of fact, we find that the velocity profiles of both modes are nearly parabolic, i.e., they are nearly "parallel" to each other. The associated particle velocities, however, have opposite signs. In the slow particle mode the particle moves against to the endolymph flow (counter-flow), whereas it moves with the endolymph in the cupula mode (co-flow).

We define the reduced-order model for BPPV as

$$\begin{pmatrix} \bar{u} \\ \dot{x}_p \end{pmatrix} = A_1 \begin{pmatrix} \bar{u}_s \\ -\sigma_s \hat{x}_{p,s} \end{pmatrix} e^{-\sigma_s t} + A_2 \begin{pmatrix} \bar{u}_c \\ -\sigma_c \hat{x}_{p,c} \end{pmatrix} e^{-\sigma_c t} \quad (21)$$

where we replaced the (nearly parabolic) velocity profile $u(r,t)$ by the bulk velocity $\bar{u}$. The vectors $(\bar{u}_s, -\sigma_s \hat{x}_{p,s})$ and $(\bar{u}_c, -\sigma_c \hat{x}_{p,c})$ are the eigenvectors of the slow particle mode and the cupula mode, respectively. The constants A_1 and A_2 are determined from the initial conditions, i.e., from the particle and endolymph velocity immediately after the head maneuver has ended.

It is straightforward to show that

$$A_1 = \frac{\dot{x}_{p,0}}{-\sigma_s \hat{x}_{p,s}} \frac{\theta_0 - \theta_c}{\theta_s - \theta_c} \quad (22a)$$

$$A_2 = -\frac{\dot{x}_{p,0}}{-\sigma_c \hat{x}_{p,c}} \frac{\theta_0 - \theta_s}{\theta_s - \theta_c} \quad (22b)$$

where $\theta_0 = \bar{u}_0/\dot{x}_{p,0}$ is the ratio between the initial fluid and particle velocities, and θ_s, θ_c are the corresponding ratios for the slow particle and cupula mode, respectively.

Numerical simulations show that typical head maneuvers end with negative fluid and particle velocities. Therefore, we can assume a co-flow situation at $t = 0$ ($\theta_0 > 0$). On the other hand, we have found at the end of the previous section that the slow particle mode (counter-flow) will always prevail as $t \to \infty$. Therefore, either the fluid flow $\bar{u}$ or the the particle velocity $\dot{x}_p$ must change sign at a certain time $t > 0$. These two cases are shown schematically in Figure 8.

The case $A_1 > 0$ describes BPPV. Here, the cupula relaxes faster than the particles fall to the bottom of the canal. The fluid velocity will change sign at $t = T_P$ which is the time of the peak nystagmus and $|V| = V_{\max}$.

For $A_1 < 0$ the fluid velocity remains negative for all $t > 0$ and only the particle velocity changes sign. In that case the particles fall faster than the cupula relaxes. There is no nystagmus. Although theoretically possible, we have not been able to observe this case in our numerical simulations of the full nonlinear equations.

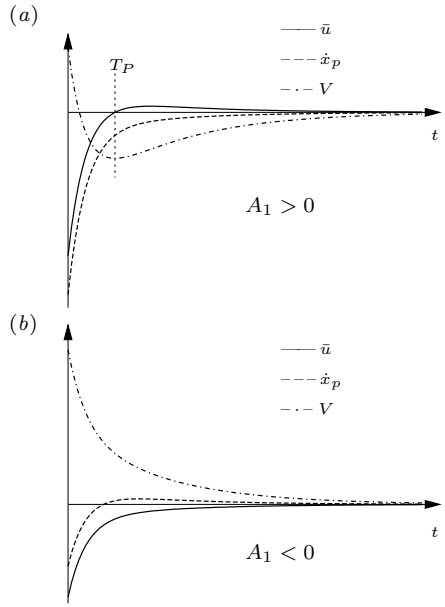

Figure 8: Two possible cases of transition from co-flow to counter-flow: (a) for $A_1 > 0$ the fluid velocity $\bar{u}$ changes sign at $t = T_P$; (b) for $A_1 < 0$ the particle velocity $\partial x_p/\partial t$ changes sign and there is no positional nystagmus.

The reduced-order model allows us to derive explicit (approximate) expressions for the characteristic values of the positional nystagmus (T_L, T_P, and $V_{\max}$). For example, the time to peak T_P (where the endolymph bulk velocity $\bar{u}$ changes sign) is given by

$$T_P = \frac{1}{\sigma_c - \sigma_s} \ln \left[\frac{\theta_c(\theta_0 - \theta_s)}{\theta_s(\theta_0 - \theta_c)} \right] \quad (23)$$

With the help of the function θ_u we can further simplify the expressions for T_P, T_L, and $V_{\max}$.

$$\theta_u = \frac{-\chi Fr^2 \xi}{\epsilon Fr^4 \xi^2 - (16 + 2\chi) Fr^2 \xi + 4} \quad (24)$$

The function θ_u approximates θ_s for $St < 1$ and θ_c for $St > 1$. The change from co- to counter-flow is reflected by a change of sign of θ_u as St passes through unity. With this we obtain the simplified explicit expressions for the characteristic values of the positional nystagmus:

$$T_P = \frac{16}{\epsilon} \frac{St}{St - 1} \ln \left(1 - \frac{\theta_0}{\theta_u} \right) \quad (25a)$$

$$T_P - T_L = \frac{16}{\epsilon} \frac{St}{St - 1} \ln St \quad (25b)$$

$$V_{\max} = \frac{16}{\epsilon} \bar{u}_0 (St - 1) \left(1 - \frac{\theta_0}{\theta_u} \right)^{-\frac{1}{St-1}} \quad (25c)$$

We have tested the expression for $T_P - T_L$ against numerical simulations of the linearized equations (15) and of the full nonlinear BPPV model (11). According to (25b) the difference between latency and time to peak is independent of the number of particles. We see from figure 9 that (25b) is a good prediction for $T_P - T_L$ for large particles ($St < 1$). For small particles ($St > 1$) the influence of n_p becomes visible and expression (25b) under-predicts $T_P - T_L$. Apparently, the nonlinear gravity term plays a larger role for small particles.

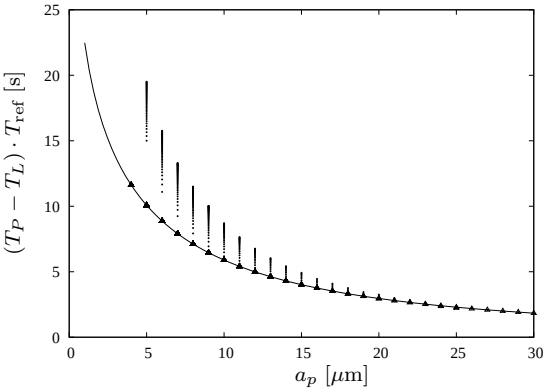

Figure 9: Difference between the time to peak T_P and the latency T_L (—— expression (25b); • nonlinear simulation, $n_p = 1, \ldots, 50$; ▵ linear simulation, $n_p = 1, \ldots, 50$).

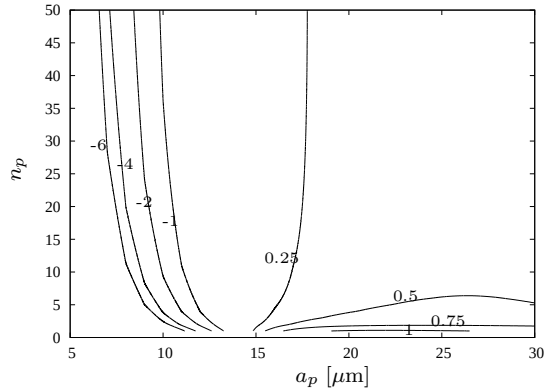

Figure 10: Ratio θ_0/θ_u as a function of the particle size a_p and number n_p (values indicated at the contour lines).

The expression (25b) can be evaluated without knowing anything about the head maneuver. The expression (25a), however, requires knowledge of the initial condition θ_0, i.e., the result of the head maneuver. In Figure 10 we have plotted the ratio θ_0/θ_u obtained from numerical simulations of the nonlinear equations. For small particles ($St > 1$) the ratio is negative and it becomes more negative the smaller the particles get. According to (25a) the cupula displacement then peaks at increasingly later times T_P. For large particles ($St < 1$) and large n_p the behaviour remains qualitatively the same. For small numbers of larger particles, however, we find that the ratio θ_0/θ_u approaches 1. It becomes even larger than 1 for $n_p = 1$ and $a_p \approx 20 \ldots 25\mu$m. In that case there should be no positional nystagmus (compare to figure 8(b) where the particle velocity changes sign rather than the fluid velocity). However, in the nonlinear case these effects are somewhat mollified and we have not been able to observe the disappearance of the positional nystagmus.

CONCLUDING REMARKS

A central result of our study is the formulation of several dimensionless coefficients which determine the behavior of SCC with canalithiasis. The reduced-order model is a simple model with two degrees of freedom which describes the post-rotatory phase ($t > 0$) as an initial value problem. The expressions (25) are a direct result of this model. They allow us to study the influence of geometrical parameters (e.g., canal radius, particle size, etc.) on BPPV.

We find, for instance, that the latency T_L and the time to peak T_P are proportional to R. This simple result leads to a possible explanation for the clinical observation that patients with canalithiasis in the horizontal SCC (< 10% of all cases) show shorter latency and a stronger and earlier nystagmus than patients with canalithiasis in the posterior SCC (∼ 90% of all cases). At least the shorter latency and the earlier peak nystagmus can be explained by the canal geometry: the major radius R of a typical horizontal SCC is approximately 10 to 20% smaller than in the posterior canal (Curthoys *et al.*, 1976).

The proposed model is able to explain the principal relations between the physical and geometrical parameters and the BPPV symptoms. However, it is not able to predict precisely the intensity of the positional nystagmus, for instance. We assume that the biggest difference between our model and the actual physiological process lies in the particle modeling. Our particle model assumes Stokes drag in a flow field without walls. However, the pressure drop due to a (very small) sedimenting particle in a pipe is a function of the radial position of the particle (see, e.g., Happel & Brenner, 1973; Squires *et al.*, 2004). Our model under-predicts the pressure drop if the particle is in the center of the canal, and it over-predicts the pressure drop if the particle is close to the wall. To study this effect we added an equation of motion for the radial direction to our governing equations. We found that the particles spend most of the time during the head maneuver ($t < 0$) and after the peak nystagmus ($t > T_P$) close to the wall. During the phase where the positional nystagmus is building up ($0 < t < T_P$), the particles are mostly close to the center of the canal. So, it turns out that our crude particle model yields (on average) the correct pressure drop. We also found that the results remain qualitatively the same whether we include the radial equation of motion or not. The inability of our model to yield good predictions for the nystagmus intensity (compare, for instance, figures 2 and 4) is most likely due to the fact that we neglect the blockage effect of large particles ($a_p/a > 0.1$) and the effect of clusters of sedimenting particles.

REFERENCES

Curthoys, I. S., Markham, C. H., and Curthoys, E. J., 1976, "Semicircular duct and ampulla dimensions in cat, guinea pig and man", *J. Morph.*, Vol. 151, pp. 17–34.

Happel, J., and Brenner, H., 1973, "Low Reynolds Number Hydrodynamics: with special applications to particulate media", 2nd edn., Noordhoff, Leyden.

Obrist, D., 2007, "Fluidmechanics of semicircular canals – revisited", *ZAMP*, submitted.

Rajguru, S. M., Ifediba, M. A., and Rabbitt, R. D., 2004, "Three-dimensional biomechanical model of benign paroxysmal positional vertigo", *Ann. Biomed. Eng.*, Vol. 32 (6), pp. 831–846.

Rajguru, S. M., Ifediba, M. A., and Rabbitt, R. D., 2005, "Biomechanics of horizontal canal benign paroxysmal positional vertigo", *J. Vest. Res.*, Vol. 15, pp. 203–214.

Squires, T. M., Weidmann, M. S., Hain, T. C., and Stone, H. A., 2004, "A mathematical model for top-shelf vertigo: the role of sedimenting otoconia in BPPV", *J. Biomech.*, Vol. 37, pp. 1137–1146.

Van Buskirk, W. C., Watts, R., and Liu, Y., 1976, "The fluid mechanics of the semicircular canals", *J. Fluid Mech.*, Vol. 78 (1), pp. 87–98.